# Looking back over the shoulder : new insights on the unique scapular anatomy of the tapir (Perissodactyla: Tapiridae)

TITLE

# Looking back over the shoulder: new insights on the unique scapular anatomy of the tapir (Perissodactyla: Tapiridae)

**Jamie A. MacLaren[1,2]***

**Affiliation:**

[1] Department of Biology, Universiteit Antwerpen, Building D, Campus Drie Eiken, Universiteitsplein, Wilrijk, Antwerp, 2610, Belgium.

[2] Evolution & Diversity Dynamics Lab, UR Geology, Université de Liège, 14 Allée du 6 Août, 4000 Liège, Belgium.

**Corresponding Author:** Jamie A. MacLaren, Room D1.41, Building D, Campus Drie Eiken, Universiteitsplein 1, 2610 Antwerp, Belgium.

**ORCID**: orcid.org/0000-0003-4177-227X

**Correspondence Email:** jamie.maclaren@uantwerpen.be

**Correspondence Telephone:** (+32) 487774980

**Abstract**

The musculoskeletal anatomy of the shoulder of many ungulates has been inferred from veterinary model taxa, with uniformity in muscle arrangements and attachment sites often assumed. In this study, I investigated the muscular and osteological anatomy of tapirs and their relatives (Perissodactyla: Tapiroidea), using a combination of gross dissection and digital imaging (photography and laser surface scanning). Dissections of three modern tapir species revealed that the *m. infraspinatus* originates from both supraspinous and infraspinous fossae for all species, lying on both sides of the distal scapular spine. The epimysial border between the *m. supraspinatus* and *m. infraspinatus* origin sites is marked in all species by an ossified ridge, sometimes extending the length of the scapular spine. This 'supraspinous ridge' is clearly visible on the scapular surface of both modern and extinct *Tapirus* scapulae; however, the ridge does not appear present in any non-*Tapirus* tapiroids examined (e.g. *Helaletes*, *Nexuotapirus*), nor in other perissodactyls or artiodactyls. Moreover, the ridge exhibits a clearly distinct morphology in *T. indicus* compared to all other *Tapirus* species examined. Combined, these findings indicate that the presence and position of the 'supraspinous ridge' may represent a robust phylogenetic character for reconstructing relationships within tapiroids. Unfortunately, any functional locomotor outcomes or benefits of the *m. infraspinatus* straddling the scapular spine remains elusive. This study represents a firm reminder for anatomists, veterinarians, and palaeontologists to (where possible) look beyond veterinary model systems when inferring musculoskeletal form or function in non-model organisms.

## Introduction

Our understanding of mammalian gross anatomy has often been driven by in-depth qualitative and quantitative assessments of veterinary model species (e.g. horses, cattle, cats and dogs) (Böhmer et al., 2020; Budras et al., 2012; Liebich et al., 2007; Liebich & König, 2020). In recent years, investigations into the musculoskeletal anatomy of the appendicular skeleton of poorly known mammal groups has become more prevalent. Such investigations include those of close relatives to traditional veterinary models (e.g. pantherine cats: Cuff et al., 2016; African wild dogs: Smith et al., 2020; etc.), but also include a wide array of taxa which deviate from the morphology of well-known veterinary model species, such as xenarthrans (Diniz et al., 2018; Nyakatura & Fischer, 2011), monotremes (Regnault & Pierce, 2018), and a diverse array of ungulates including giraffes, camels, reindeer, rhinoceroses, and tapirs (Etienne et al., 2021; Graziotti et al., 2012; MacLaren & McHorse, 2020; Martini et al., 2018; Onwuama et al., 2021). A quantitative understanding of modern groups which phylogenetically bracket extinct taxa can be useful to investigate functional anatomy and infer behaviour in the fossil record (e.g. Nyakatura et al., 2019; Toledo et al., 2013; Witmer, 1995). Such investigations yield information on the comparative structure and potential function of the appendicular muscles as they act on the skeleton, both of which may be highly derived (e.g. sloths; Olson et al., 2018; Toledo et al., 2013). In some cases, this may raise questions on the adaptive or functional benefits for a specific muscular arrangement or skeletal morphology through the evolution (or ontogeny) of the organism.

A recent study on the forelimb muscular architecture of the Malayan tapir (*Tapirus indicus* Desmarest) in comparison to modern domestic horses (*Equus ferus caballus* Linneaus) showed a peculiar additional belly to the *m. infraspinatus* (lateral shoulder stabiliser; Budras et al., 2012; MacLaren & McHorse, 2020), with a corresponding divergence in scapula skeletal morphology compared to other tapir species (MacLaren & McHorse, 2020; MacLaren & Nauwelaerts, 2016). In this example, the scapular spine (*spina scapulae*) of *T. indicus* is deflected caudally, with a strong ridge along the cranial surface of the scapular spine. This hitherto undescribed ridge was shown to represent an osteological indicator for the boundary between *m. supraspinatus* and *m. infraspinatus* muscles, with the *m. infraspinatus* of *T. indicus* invading the cranial surface of the scapula spine (MacLaren & McHorse, 2020). Previous published reports of *T. indicus* muscular anatomy (e.g. Bressou, 1961) noted the unusual arrangement of the muscles, but did not detail the morphology of the bone or comment

on the functional or comparative morphology further. The ridge is identified as a “muscular line” in an account of a Pleistocene tapir from South America (Holanda et al., 2012), but again this line was not elaborated upon as regards its potential function, or even what it represented other than a ridge where a muscle attached in life. MacLaren and Nauwelaerts (2016) noted the ridge was present in the scapula of tapirs, but again refrained from elaborating on its potential function. MacLaren and McHorse (2020) noted and quantified the morphology and architecture of the *m. infraspinatus* muscle in two different *T. indicus* specimens of differing ages, both presenting the same bony ridge on the scapular spine and the same muscular arrangement (MacLaren & McHorse, 2020). Limb dissections of other extant species of tapir (e.g. *Tapirus terrestris* Linneaus;Campbell, 1936; Pereira et al., 2015) did not report the same musculoskeletal arrangement. As such, the layout of the lateral muscles of the tapir shoulder remain somewhat ambiguous in their arrangement, origins, and possible links to skeletal morphology or limb function.

In this study, I use a combination of detailed dissection of forelimbs from three species of modern tapir (*Tapirus indicus*, *T. terrestris* and *T. pinchaque* Roulin) and three-dimensional surface scans of scapulae from a range of tapiromorph species (both extant and extinct) to investigate the morphology of the scapula of this enigmatic group. Based on previous dissection reports, I expected the muscle arrangement of the deep lateral muscles (*m. supraspinatus* and *m. infraspinatus*) in the tapir forelimb would follow the pattern exhibited by other ungulates (e.g. horses, bovids, suids, giraffids, cervids, rhinocerotids; Budras et al., 2012; Etienne et al., 2021; Liebich & König, 2020; Onwuama et al., 2021; Wareing et al., 2011), and that the Malayan tapir *T. indicus* would represent an anomalous muscular arrangement as previously noted in Bressou (1961) and MacLaren and McHorse (2020). For the first time, I describe the presence and interspecific variability in the location of a notable ridge expressed on the cranial surface of the tapir scapula delineating the separation of two muscles, with no clear analogues in other ungulates, and I attempt to provide functional and evolutionary interpretations within a phylogenetically informed framework.

## Material and Methods

*Cadaver Dissections*

Five forelimb cadavers representing three species of tapir (two *Tapirus indicus*; one *T. terrestris*; and two *T. pinchaque*) were dissected (Table 1). *Tapirus indicus* specimens (Qadira and Kamal; Figure 1A) were donated by the Koninklijke Maatschappij Dierkunde Antwerpen (KMDA) to the Museum Morfologie (Universiteit Gent), with cadaver dissection performed at the Laboratory of Applied Veterinary Morphology of the Universiteit Antwerpen. The *T. terrestris* specimen (Torbjörn; Figure 1B) was culled following ethical guidelines at the Kolmården Wildlife Park, Sweden. Published material from previous dissections of *T. terrestris* (Pereira et al. 2015) was also inspected. The *T. pinchaque* specimens (Carlotta and Cofan; Figure 1C; Table 1) were donated to the Denver Museum of Nature and Science (DMNS) by the Cheyenne Mountain Zoo following death by natural causes, with cadaver dissections performed at the DMNS Zoology Lab. One specimen (Qadira) was considered a juvenile (5 months; Table 1); tapirs in this study are considered mature beyond two years of age (following the trend exhibited in equids; Rogers et al., 2021). Full skeletal maturity (full epiphyseal ossification) was achieved only in Kamal, Carlotta and Cofan. Patterns of skeletal maturity are further complicated by the effect of nutrition on delaying ossification in ungulate mammals, which can occur more frequently in captive animals (Flinn et al., 2013). Young and old specimens of *T. indicus* exhibited very similar muscle arrangements (MacLaren and McHorse, 2020; this study), and as such the specific morphology of the scapula in question appears to be both a juvenile and adult feature.

Skin and fascia were removed from the shoulder region, and the lateral shoulder muscles were carefully removed from the skeleton, with particular attention paid to the origin of the supraspinatus (*m. supraspinatus*), infraspinatus (*m. infraspinatus*) and deltoid (*m. deltoideus pars scapularis*) muscles (Figure 1). Dissections were performed with assistants present to verify on-the-spot observations, with photographic documentation of much of the dissection. More details and photographic documentation can be found in Supplementary Information 1: Additional Dissection Information, Figures S1-S6.

*Scapula Specimens*

Scapulae of 48 specimens across 14 species of tapiromorphs were collected from various museum collections and digitised using a laser surface scanner, or structure-from-motion photogrammetry, or two-dimensional

photographic images (Table S1). Laser scans were taken using a FARO Platinum V2 laser ScanArm with an integrated LaserLine probe, with scans of *Tapirus lundeliusi* Hulbert taken using an Artec Spider. Structure-from-motion models were compiled from 2D images taken with a Nikon D3000 DSLR camera for a specimen of *Helaletes* sp.. Models were built in RealityCapture (v. 1.2.1.116300; RC Epic Games Slovakia, 2023). Scapulae with the full lateral surface, encompassing the complete two lateral fossae, were preferred; however, certain features of the scapula detailed in this study are also visible on broken scapulae preserving only the ventral angle (glenoid fossa and distal scapular spine). The scapula condition and specimen numbers are provided in Supplementary Information 2: Specimen List (Table S1), with 3D models visualised in lateral aspect in Supplementary Information 3: Scanned Scapula Specimens, and the models available publicly on MorphoSource project ID: 000505274. Additional 2D images of scapulae which were unavailable for scanning but exhibited key features pertinent to this study were sourced from published articles and photographs of museum specimens (see Table S1).

*Cross-sectional Scapula Fossa Ratio*

The lateral muscles of the scapula (*m. supraspinatus* and *m. infraspinatus*) are essential for shoulder stability in ungulates. Quantifying their attachment areas may be used as a proxy for the importance of these muscles within the locomotor system of the animal (MacLaren & Nauwelaerts, 2016). The ratio of scapular fossa areas has been used to investigate ungulate shoulder anatomy in recent years (MacLaren & Nauwelaerts, 2016; Van Houtven & MacLaren, 2019). I adapt this method to measure linear distances on two-dimensional cross-sectional models derived from 3D scans. 2D analyses were favoured to enable the inclusion of species and specimens with incomplete scapulae (e.g. *Tapirus webbi*; Supplementary Information 3). Cross-sections were taken in the open-source freeware Blender (v. 3.0.0); sections were recorded perpendicular to the scapular spine and immediately distal to the tuber of the scapular spine (*tuber spinae scapulae*) (Figure 2A). Orthographic images of these cross-sections were taken in MeshLab (v. 2022.02) using the "Save snapshot" tool. The regions observed to be the origins of *m. supraspinatus* and *m. infraspinatus* muscles (based on comparative dissections, see above) were then measured on the orthographic images using the segmented line tool in ImageJ (v. 1.53k) (Figure 2B) and compared between species (Figure 2C). The ratio of *m. supraspinatus* to *m. infraspinatus* origin

immediately prior to the *tuber spinae* was adapted for linear measurements from the three-dimensional scapular fossa ratio (SFR) calculation in MacLaren and Nauwelaerts (2016): $L_{supra} \div (L_{supra} + L_{infra})$. Origin cross-sectional (CS) length measurements were exported into the R statistical environment (R Core Team, 2020), where the raw values were visually compared using a biplot, SFR values per species inspected using a boxplot, and resultant SFR calculations analysed for significant differences. Full scapula scans and CS segment scans are available publicly from the MorphoSource project ID: 000505274

*Scapula Fossae Topography*

Visual observation of the surface of the scapula or the cross-sections did not always show clearly where the features of interest appeared on the scapula. The surface of the lateral scapular fossae were therefore assessed using the 'molaR' package (v. 4.0; Pampush et al., 2016) to visually inspect the supraspinous fossa surface using Dirichlet Normal Energy (DNE). Dirichlet Normal Energy has been used as a characterisation of topographical complexity for a variety of biological features (e.g. Gardiner et al., 2018; Waldman et al., 2023), and here I use it to visually highlight features of the scapula surface. The surface scans of scapulae (both complete and partial) were decimated to 100k polygons in Geomagic Wrap 2017 (v. 2017.1.0.19, 3D Systems Inc.) and exported as PLY files. Since DNE can be sensitive to variations in surface mesh composition (Pampush et al., 2016; Spradley et al., 2017), I chose to re-mesh the surface models of the lateral scapula surfaces using Geomagic Wrap 2017 to produce near-isotropic meshes, all comprised of 100k polygons. Moreover, this method is used only to visually inspect and highlight morphological features in this study, rather than to extract quantitative DNE values per region or per model. In this way, variation in surface topologies can be visualised without skewing quantitative data with potentially non-comparable surface meshes. Surface-coloured scapulae were extracted, detailing the supraspinous surface morphology and snapshots taken in MeshLab for all species with 3D data available. Coloured scapula scans are available publicly from the MorphoSource project ID: 000505274.

*Statistical and Phylogenetic Analyses*

Boxplots were used to visually inspect the range of SFRs exhibited by each species, including species with only one scapula available (*Tapirus lundeliusi* and *T. webbi* Hulbert). Species with only one complete individual available were not used to test for significant differences using analysis of variance (ANOVA), which thus restricted the statistical analysis to five species (four extant, one extinct). Welch's ANOVA was chosen to reduce likelihood of Type-1 errors in the analysis, given the uneven sampling. Post-hoc testing for multiple comparisons was performed using both a Games-Howell test (to further avoid Type-1 errors) and pairwise t-tests with p-values adjusted using the Bonferroni-Holm correction to account for multiple simultaneous tests (alpha = 0.05).

Phylogenetic trait mapping was conducted for visually inspecting the evolution of novel features in the scapula of tapiroids (Tapiridae plus closest outgroups). I used a composite tree (built in Mesquite v.3.81) based on interspecific relationships published in the most recent tapirid phylogenies (Cozzuol et al., 2013; Holanda & Ferrero, 2013; Hulbert, 2010), further adapted from MacLaren et al. (2018). Fourteen tapiroid taxa were chosen, based on scapula material available for inspection from both 3D scans and 2D images with sufficient resolution to observe scapula features. The composite tree was time-scaled using the *paleotree* v. 3.3.25 package (Bapst, 2012) in R-Studio (2023.06.1; RStudio Team, 2020), based on first-last appearance dates extracted from the Paleobiology Database and supplemented from published literature (Cozzuol et al., 2013; Franzen, 2010; Padilla et al., 2010; Qiu et al., 1991). The resultant time-calibrated tree preserves a monophyletic *Tapirus*, with *T. indicus* separate from neotropical taxa. The nexus file, phylogeny, and R-code used for performing phylogenetic analyses can be found in the Supplementary Information 4: R-code & Inputs. The condition of the scapula was plotted onto the composite tree, and the trait values visualised using the 'simmap' function in the *phytools* v. 0.7-90 R package (Revell, 2012), producing a colour-coded tree visually tracking presence/absence of certain features of the scapula through the tapiroid phylogeny. Ancestral states were not extracted from this analysis; results were used only to visualise the changes in scapula morphology and draw inferences in an evolutionary context.

## Results

192 *Muscle Arrangement*

193 Comparative dissections of the shoulder region of three extant species of tapirs (*Tapirus indicus, T. terrestris,*
194 and *T. pinchaque*) suggest a high level of homology between muscle originations and general morphology. The
195 shoulder muscles of *Tapirus indicus* are described in detail in MacLaren and McHorse (2020); for the purposes
196 of this study, the three intrinsic muscles of the limb which attach around the scapular spine (*m. supraspinatus,*
197 *m. infraspinatus,* and *m. deltoideus*) are compared between the three species (Figure 3):

198 Supraspinatus – the *m. supraspinatus* is a large muscle in all three species, originating from the cranial
199 region of the lateral scapula and passing over the suprascapular notch to insert on the greater tubercle.
200 Origination on the scapular blade in *T. indicus* encompasses almost the entire supraspinous fossa, meeting the
201 accessory belly of the *m. infraspinatus* on the cranial surface of the scapular spine, denoted by a strong ridge
202 along the cranial surface of the scapular spine (Figure 3a). The scapular spine is caudally deflected (often
203 strongly) at the ridge (from here termed the 'supraspinous ridge'). Origination of the *m. supraspinatus* on the
204 scapular blade of both *T. pinchaque* and *T. terrestris* encompasses approximately two thirds of the supraspinous
205 fossa, meeting the accessory belly of the *m. infraspinatus* at a supraspinous ridge which extends from a point
206 level with the distal margin of the scapular spine and terminates at the proximal margin of the scapula (Figure
207 3b,c). The scapular spine shows little or no caudal deflection.

208 Infraspinatus – the *m. infraspinatus* is a very large muscle in all three species, originating as two
209 somewhat indistinct bellies across the caudal region of the scapula and inserts strongly on the greater tubercle,
210 distal along the humeral body to the *m. supraspinatus* insertion, and proximal to the insertion of the teres minor.
211 Origination of the main belly on the scapular blade of all three species encompasses the entire infraspinous
212 fossa, including much of the caudal aspect of the scapular spine. The accessory belly of the *m. infraspinatus* is
213 poorly defined from the muscle tissue of the main belly; it shares so many fibres with the main belly that defining
214 it as a 'belly' is itself somewhat questionable. The accessory belly of *T. indicus* originates from the deflected
215 region of the scapular spine, caudal to the supraspinous ridge, and passes over the rest of the distal scapular
216 spine. The accessory belly of both *T. terrestris* and *T. pinchaque* invades the supraspinous fossa and originates
217 from approximately one third of the supraspinous fossa and the cranial aspect of the scapular spine. Thus, in all
218 three species, the *m. infraspinatus* bridges the scapular spine distal to the *tuber spinae*, and divides its origins

either side of the *tuber spinae*, where the scapular belly of the *m. deltoideus* originates. The 'supraspinous ridge' is very clear in older individuals (e.g. *T. pinchaque* specimen Carlotta, 28 years old), but was clearly present in all specimens investigated, exhibiting three clear morphologies: no ridge at all; a ridge on the cranial aspect of the scapular spine; and a ridge dividing the supraspinous fossa.

Deltoideus – the *m. deltoideus* of all three species of tapir appeared with two distinct bellies. The main belly originates as an aponeurosis across the *m. infraspinatus*, transitioning to a large muscular belly covering the distal *m. infraspinatus* and *m. teres minor*. The secondary belly (observed here and in MacLaren and McHorse (2020), but not described in the latter) arises from the *tuber spinae* with a strong tendinous attachment, then passes over the *m. infraspinatus* to insert alongside the main belly, both on the deltoid tuberosity of the humerus. The morphology of this second *m. deltoideus* belly is reminiscent of the acromion belly of the *m. deltoideus* in artiodactyls and carnivorans, although genuine homology can only be speculated here without a greater comparative or ontogenetic sample. All features of the *m. deltoideus* muscles were present in all three species.

Gross dissection of the shoulders of the three modern tapir species specifically highlight the dimorphic nature of the supraspinous ridge when present. When tapiroids outside the genus *Tapirus* were inspected, no evidence of a ridge on the supraspinous fossa surface was found. When trait conditions were visualised on the composite phylogeny, the origin of the supraspinous ridge (both the scapula spine morph (only *T. indicus*) and the supraspinous fossa surface morph) appears to fall at the origin of the genus *Tapirus* (Figure 3d). The sister taxon to *Tapirus* in most analyses (*Plesiotapirus yagii* Qiu et al.) does preserve a scapula, but it is poorly digitised (Qiu et al., 1991) and so the supraspinous ridge feature can neither be confirmed nor rejected for this taxon (Figure 3d). In the case of *Tapirus arvernensis* Croizet & Jobert, hypothesised as the sister species to *T. indicus*, visual inspection of published images (Grandi et al., 2023) are inconclusive as to the presence of a supraspinous ridge (as reflected in Figure 3d). Given that no species prior to the origin of *Tapirus* exhibits a supraspinous ridge, from here the results will focus on quantifying the differences in the supraspinous ridge of the *Tapirus* scapula.

245 *Cross-sectional Scapular Fossa Ratios*

246 Cross-sectional lengths (CSLs) of the *m. supraspinatus* and *m. infraspinatus* attachment sites (inferred from
247 comparative dissections) were visualised in a bivariate morphospace (Figure 4a). *Tapirus indicus* exhibits
248 notably different morphospace occupation to all other tapirs in the quantitative study, with very high values for
249 the *m. infraspinatus* compared to other species. The other modern taxa (*T. bairdii* Gill, *T. terrestris* and *T.*
250 *pinchaque*) plot together with the dwarf tapir *T. polkensis* Olsen (from late Neogene of North America) in the
251 lower section of the morphospace, indicating substantially smaller *m. infraspinatus* CSLs in these species. The
252 solitary specimens of *T. webbi* and *T. lundeliusi* (from the late Neogene of Florida) plot apart from the cluster
253 of modern Neotropical species plus *T. polkensis*, suggesting much larger *m. supraspinatus* CSLs compared to
254 modern taxa but notably lower *m. infraspinatus* CSLs than *T. indicus* (Figure 4a).

255 Two-dimensional scapula fossa ratios (2D-SFRs) for the above species were visually inspected using a boxplot
256 (Figure 4b) and tested for significant differences between groups using a one-way ANOVA and post-hoc
257 comparisons (Table 2). The 2D-SFRs of *T. indicus* were significantly higher than those of other species (Table
258 2), with the exception of *T. pinchaque* when using Games-Howell post-hoc testing ($p = 0.089$). The non-
259 significant t-test results were comparisons between *T. polkensis* and *T. terrestris* ($p = 0.196$) and *T. bairdii* and
260 *T. pinchaque* ($p = 0.719$), with the comparison between *T. pinchaque* and *T. terrestris* trending toward
261 significance but not fully supported ($p = 0.054$). No significant differences were recovered using Games-Howell
262 post-hoc testing for *T. polkensis*. The significant differences between *T. polkensis* and other modern tapir taxa
263 recovered via t-tests must also be considered with caution, given the low sample size for *T. polkensis* (n=2). The
264 lack of multiple well-preserved specimens of *T. webbi* and *T. lundeliusi* precluded significance testing between
265 these two species and those which were represented by more than a single specimen. No significant differences
266 were detected between modern Neotropical species (Table 2).

267

268 *Scapula Topographical comparison*

269 Topographical analysis using Dirichlet Normal Energy (DNE) highlighted the supraspinous ridge of exemplar
270 specimens in most cases (Figure 5a-i). The supraspinous ridge is expressed to varying degrees of prominence

271 in scapulae of different *Tapirus* species, although the arrangement is always consistent within a species (see
272 Figure 3d; see also Supplementary Information 3: Scanned Scapula Specimens). Angled lighting on 3D models
273 added additional qualitative evidence for the position of the supraspinous ridge, bisecting the supraspinous fossa
274 in all *Tapirus* species with the exception of *T. indicus*, where the ridge arises from from the scapular spine
275 (Figure 3a; Figure 5a). For specimens where topographical analysis was not possible (e.g. *Nexuotapirus*,
276 '*Hyrachyus'*), 2D images were inspected, with no ridge found. These images do not entirely preclude the
277 presence of a supraspinous ridge. However, it is unlikely that such a conspicuous ridge (which extends to the
278 glenoid apex of the scapula spine in *Tapirus* spp.) would not be at all visible from more detailed lateral images
279 (e.g. *Nexuotapirus*, Figure 5j). Images of the Urtapir '*Hyrachyus' minimus* (HLMD-Me 16000) from the Messel
280 Pit in Germany appear to show signs of a supraspinous ridge on the scapula spine (Figure 5k). The photographs
281 available were not of ideal quality (Figure 5k), and the phylogenetic affinity of the Messel Urtapir is in need of
282 comprehensive reappraisal. As such, no firm stance is taken on the presence or absence of a supraspinous ridge
283 in this species in this study until a full morphological and phylogenetic reassessment are available (Figure 3c).
284 The damaged *Helaletes* scapula DMNS 15399 also did not present a clear or obvious ridge on the supraspinous
285 fossa near the glenoid. As this specimen is quite fragmentary (Figure 5l), this may not be as solid a result as
286 those for *Tapirus* spp. scapulae, even though similar remains from *Tapirus* spp. (e.g. *T. veroensis* or *T. haysii*;
287 Figure 5h-i) do exhibit a supraspinous ridge along the scapula portion preserved in *Helaletes* DMNS 15399.

288

289 **Discussion**

290 In this study I have investigated the lateral shoulder musculature of tapirids, an enigmatic ungulate group with
291 several seemingly unique aspects to their scapula osteology and associated myology. Using a combination of
292 detailed dissection, three-dimensional surface scanning, two-dimensional imagery, and topographical analyses,
293 I have discovered and described a new and novel feature on the tapir scapula (the supraspinous ridge), and I
294 have shown the variation of this feature between members of living species. From dissection results and
295 phylogenetic bracketing, the shoulder anatomy of tapirs can be elucidated through the fossil record; I then
296 interpret certain features of the tapir shoulder as having originated at the base of the genus *Tapirus*, and speculate
297 on the potential function and drivers of those unique features.

The limb musculature literature available for perissodactyls (and non-veterinary ungulates in general) is not particularly extensive by comparison to that of feeding systems or for other mammalian groups (e.g. primates and carnivorans; Deutsch et al., 2020; Fabre et al., 2018; Hartstone-Rose et al., 2012; Hartstone-Rose et al., 2022; Law et al., 2022; Marchi et al., 2018; Vélez-García et al., 2018; etc.). The absence of detailed comparative limb muscle studies for large herbivore groups is not surprising, given the logistics and time constraints on performing such experiments (e.g. Böhmer et al., 2020; Etienne et al., 2021; MacLaren & McHorse, 2020), and especially if those dissections are to involve measuring quantitative muscular architecture. As a result, peculiarities in the locomotor musculoskeletal systems of numerous ungulates may have gone unidentified for centuries, and interpretations on the functional, developmental, or phylogenetic value of such peculiarities have likely been overlooked. Such is the case for the supraspinous ridge morphology in the tapir scapula, shown here to represent an osteological correlate demarcating the epimysial border between the *m. supraspinatus* and the *m. infraspinatus* in *Tapirus* (MacLaren & McHorse, 2020; this study). The available literature describing the shoulder musculature of tapirs (*Tapirus indicus*: Bressou, 1961; MacLaren & McHorse, 2020; Murie, 1872; *T. terrestris*: Campbell, 1936; Pereira et al., 2015) provide quite contrasting accounts of the arrangements of the *m. supraspinatus* and *m. infraspinatus*, even within the same species. Murie (1872) described the *m. supraspinatus* of *T. indicus* as covering the entire supraspinous fossa, as would be expected for an ungulate based on veterinary descriptions of horses, suids and bovids; however, the later description by Bressou (1961) and the quantitative assessment by MacLaren and McHorse (2020) specifically state the *m. supraspinatus* occupies the cranial section of the supraspinous fossa, whereas the *m. infraspinatus* finds origin from the remainder of the supraspinous fossa (including the cranial surface of the scapular spine) and the infraspinous fossa. This arrangement of muscles is corroborated in the present study, which used the same specimens as MacLaren and McHorse (2020), further verified by dissections of the other tapir species. Dissection reports for the shoulder region of Neotropical *T. terrestris* vary even more greatly: Campbell (1936) compared *T. terrestris* to a hippopotamid (*Choeropsis liberiensis*) and suid (*Sus scrofa*), concluding that the *m. supraspinatus* originated from the supraspinous fossa and divided into two bellies, one of which occupies the cranial supraspinous fossa and inserts over the bicipital groove (as in other ungulates). The second belly is described as originating from the supraspinous surface of the scapular spine, merging with the *m. infraspinatus* and inserting with it on the lateral greater tubercle of the humerus (Campbell, 1936). By contrast, Pereira et al.,

(2015) described the *m. supraspinatus* as occupying the entire supraspinous fossa of *T. terrestris*. It should be noted that several muscle origination and insertion sites published in Pereira et al. (2015) (and the subsequent Pereira et al., 2017) are not aligned with those reported in previous studies on tapir limb musculature (Campbell, 1936; Bressou, 1961; MacLaren and McHorse, 2020; this study) or ungulates used for veterinary study (e.g. Budras et al., 2012; Liebich and König, 2020), and thus caution must be taken when comparing the results from Pereira et al. (2015) to these other studies (including the present contribution). In summary, it is clear that prior to this study there was no consensus on the arrangement of the *m. supraspinatus* and *m. infraspinatus* in tapirs. Here, I have endeavoured to demonstrate that both *T. indicus* and *T. terrestris* (in addition to *T. pinchaque* and, by osteological inference, the remainder of the genus *Tapirus*) exhibit a *m. infraspinatus* muscle with dual origins on both sides of the scapular spine (see Figure 3), with their separation marked by a newly described osteological feature: the 'supraspinous ridge'.

The supraspinous ridge is shown here to be pervasive within all scapulae of species widely accepted to belong to the genus *Tapirus*. All *Tapirus* species exhibit a ridge separating the origin site of the *m. supraspinatus* and *m. infraspinatus* muscles, based on qualitative observation of multiple 3D scans (and figures in published articles, e.g. Holanda et al., 2012; Pereira et al., 2015; MacLaren and Nauwelaerts, 2016). The divergence in supraspinous ridge morphology into two clear and consistent modes among the *Tapirus* species is noted here for the first time. The expression of the ridge bisecting the supraspinous fossa in all examined *Tapirus* species (except *T. indicus*) leads to the inference that the deep lateral shoulder muscle arrangement present in *T. terrestris* and *T. pinchaque* is common to nearly all species of *Tapirus*, and therefore the invasion of the supraspinous fossa by the *m. infraspinatus* likely occurred very early in the evolution of the genus *Tapirus*. In the past it has been suggested that some species of *Tapirus* located more basally on the tree (Figure 3d) may belong to their own genus; these include *Tapirus polkensis* (*Tapiravus*, *sensu* Olsen, 1960; Van Der Made & Stefanovic, 2006), *Tapirus bairdii* (*Tapirella*, *sensu* Falconi-Briones et al., 2022), and *Tapirus indicus* (*Acrocodia indica*, *sensu* Groves and Grubb, 2011). The majority of phylogenetic studies on tapirs which include extinct taxa involve near-exclusively craniodental characters (Cozzuol et al., 2013; Holanda et al., 2011; Holanda & Ferrero, 2013; Hulbert, 2005, 2010), with few post-cranial characters identified as apomorphic of

specific species or groups of species within the tapir phylogeny. Given the consistently different arrangement of the lateral shoulder muscles in *T. indicus*, and the corresponding divergence in scapula spine shape (Figure 3a-c; see also MacLaren and Nauwelaerts, 2016), it may not be unreasonable to consider the supraspinous ridge as a multistate phylogenetic character for reconstructing tapir phylogenetic affinities in future studies. My own recommendation for future phylogenetic studies of tapirs would be to code the supraspinous ridge of the scapula as a character with the following character states: 0 = no ridge present; 1 = supraspinous ridge present, clearly deviating from the scapula spine; 2 = supraspinous ridge present, arising from the supraspinous fossa and clearly separate from the scapula spine. These character states should not be considered as a gradation from 0 to 2, but rather as discrete character states (evolving from state 0 to state 2 is possible without passing through state 1). Given that phylogenetic analyses of tapir interrelationships persistently lack resolution or consensus on the placement of certain taxa (including the modern *T. indicus* and *T. pinchaque*; e.g. Cozzuol et al., 2013; Holanda and Ferrero, 2013), any features found to be distinct in one taxon and consistently similar in others must be considered, even if they are not craniodental in nature. Complete evidence phylogenies would be preferable, but until such a study is undertaken it is my belief that isolated apomorphic features from both the craniodental and post-cranial skeleton (such as the supraspinous ridge) should be utilised in deciphering interspecific relationships.

Beyond the genus *Tapirus*, features resembling the supraspinous ridge do not appear consistently on the ungulate scapula. Early relatives of tapirs in North America (e.g. helaletids; Bai et al., 2017, 2019) do not appear to have displayed a supraspinous ridge (Figure 3d, Figure 5l), although further investigation is necessary before the same can be said for Eurasian taxa (e.g. Messel Urtapir '*Hyrachyus'*, *Plesiotapirus*). Looking further out in the ceratomorph phylogeny, there is no consistent evidence for this feature in rhinocerotoids either (Figure 6b). Rhinocerotids (e.g. *Dicerorhinus*, *Ceratotherium*; Figure 6b) are known to exhibit a caudally deflected scapular spine. However, the placement of the *m. deltoideus* (originating from the distal scapula spine and *tuber spinae scapulae* in rhinocerotids and tapirids; MacLaren and McHorse, 2020; Etienne et al., 2022; this study) and the enormous insertion point for the *m. trapezius* greatly expand the *tuber spinae scapulae* in rhinocerotids (Etienne et al., 2022). The absence of an 'invading' *m. infraspinatus* reported in Etienne et al. (2022) when quantifying

the musculature of *Ceratotherium* and *Rhinoceros* strongly indicates the that absence of a supraspinous ridge is a genuine signal in modern rhinocerotids. From personal observations and the few published works available (Diedrich, 2012; Handa et al., 2022; Tong & Wang, 2014), there is a feature present on the scapula of the Pleistocene rhinocerotid *Coelodonta* which is reminiscent of the supraspinous ridge. However, greater sampling and more in-depth (quantitative) investigation into the muscle arrangements of all modern rhinocerotid genera would be necessary before the feature on the scapula of *Coelodonta* could be adequately inferred as homologous with the supraspinous ridge of *Tapirus*. Beyond the Ceratomorpha within Perissodactyla, neither the equids (Figure 6c) nor the palaeotheriids (Figure 6d) exhibit any clear ridge on the supraspinous fossa of the scapula, albeit with only a small sample of very early taxa to base this conclusion on (*Sifrhippus* (n = 1), *Propalaeotherium* (n = 5), *Palaeotherium* (n = 2); MacLaren & Nauwelaerts, 2020; Wood et al., 2011). Equids have been the subjects of numerous veterinary texts detailing their extremely derived limb anatomy, which includes the absence of a fleshy head of the *m. deltoideus* passing from the *tuber spinae scapulae* (as is present in both tapirs and rhinocerotids; MacLaren and McHorse, 2020; Etienne et al., 2022; this study). I therefore tentatively hypothesise that the *m. deltoideus* of early ancestral equids likely bore resemblance to the non-monodactyl tapir and rhinoceros condition, exhibiting a smaller fleshy head with a strong origin tendon passing superior to the larger aponeurotic head originating from the lateral tendinous surface of the *m. infraspinatus* (and from the dorsal border of the scapula). Future efforts to digitally model or reconstruct basal equid (or palaeotheriid) locomotion should take this change in *m. deltoideus* layout into account when simulating the shoulder musculoskeletal apparatus.

When we look beyond the Perissodactyla to their nearest modern relatives, the Artiodactyla, there is no evidence for even a deflected scapula spine in tylopods (camels) or ruminants. Within Suina (suids and tayassuids), the scapula spine deflects caudally quite consistently across species, more so for suid scapulae (Figure 6e-f). In suids, this deflection offers the origination site for a substantial *m. deltoideus pars acromialis*, despite the absence of a true acromion in Suina (and crown perissodactyls) (Constantinescu et al., 2012), and improves the mechanical advantage for the *m. deltoideus pars scapularis* (Maynard Smith & Savage, 1956), indicating a functional role for the scapular spine deflection. Irrespective of that, no distinct ridge is present on the

supraspinous surface of the scapula of either tayassuids or suids. The only other mammalian group I was able to identify which exhibits a ridge bearing genuine similarity to the supraspinous ridge of *Tapirus* are pinnipeds, specifically otariids (sealions and fur-seals; Figure 6g) (Berta et al., 2015; King, 1983). The 'secondary scapular spine' is used as a synapomorphy of otariids within Pinnipedia phylogenetics (Berta & Wyss, 1994), although it is functionally hypothesised to define the separation of the origins of cranial and caudal bellies of the *m. supraspinatus* of otariids, rather than marking the separation of the *m. supraspinatus* and *m. infraspinatus* origination sites (English, 1976, 1977). In the otariid condition, the two *m. supraspinatus* bellies originating either side of the scapular ridge (*sensu* English, 1977; 'secondary scapula spine' *sensu* Berta and Wyss, 1994) meet to attach onto the proximal humerus, straddling the greater tubercle and inserting anterior to the *m. infraspinatus*; the tapirid condition is similar for the insertion of the *m. supraspinatus*, with the *m. infraspinatus* and *m. supraspinatus* clearly separate at origin and insertion (MacLaren and McHorse, 2020; this study). The ridge in otariids likely offers sturdy attachment for the separate bellies of the *m. supraspinatus* as it supports the shoulder during underwater propulsion and likely play a role in fine rotary control of the forelimb (English, 1977). As such, evolutionary homology of the *Tapirus* supraspinous ridge with the otariid 'secondary scapula spine' seems extremely improbable, although functional homology appears likely given the similarities in placement and morphology of both these ridge-like structures.

The method for quantifying the differences in *m. infraspinatus* and *m. supraspinatus* origin area in this study was adapted from similar methods used in previous assessments of perissodactyl scapula morphology (MacLaren & Nauwelaerts, 2016; Van Houtven & MacLaren, 2019). Prior knowledge of the extent to which the *m. infraspinatus* origin extended into the supraspinous fossa was not previously available, e.g. MacLaren and Nauwelaerts (2016) published their three-dimensional assessment of the scapula fossa ratio (SFR), with results suggesting that Neotropical tapirs exhibited a very large supraspinous fossa (and inferring a very large *m. supraspinatus*). In the present study, I have found that the *m. supraspinatus* muscle origin site cannot be assumed to encompass the entire supraspinous fossa, at least not in *Tapirus*. Results from quantitative dissections of tapirs and rhinocerotids, in addition to well established domestic equid muscle arrangements, now provide a more accurate view on the origination regions of the *m. supraspinatus* and *m. infrasinatus* of

perissodactyls, enabling an updated phylogenetic comparison between modern perissodactyl groups to be made (Figure 7; adapted from Figure 3 in MacLaren and Nauwelaerts, 2016). Remarkably, there is no published muscular architecture data for the *m. infraspinatus* of *Equus caballus* (arguably the 'model species' for anatomical and physiological studies of perissodactyls). Moreover, despite recent advances in developmental analyses of equid distal limbs (Kavanagh et al., 2020), there are to date no pre-natal or foetal developmental studies focussing on the Equus upper limb. As such, there is little by way of developmental understanding for the arrangement of the lateral shoulder muscles in perissodactyls, although evidence from other taxa suggest the scapula fossae are formed very early on in development (Großmann et al., 2002).

When visualised using the modified method in this study, and accounting for new information on tapirid and rhinocerotid shoulder musculature (MacLaren and McHorse, 2020; Etienne et al., 2022; this study), an inversed yet similar pattern is revealed within perissodactyls, with Neotropical tapirs in fact demonstrating noticeably smaller origination sites for the *m. supraspinatus* than are present in either modern equids or rhinocerotids (Figure 7). I therefore posit that assessments of scapula fossa areas, and more broadly any other inferences based on muscle attachment sites across the vertebrate skeleton, should be coupled with detailed gross dissection wherever possible (within the scope of individual financial and infrastructural constraints). In this manner, inferences on the musculoskeletal anatomy and functional morphology of both living and extinct organisms can be more accurately and reliably constructed. Indeed, at this stage the functional outcome of the *m. infraspinatus* wrapping around the scapula spine in *Tapirus* spp. can only be speculated at. It is possible that this arrangement confers greater stability to the shoulder joint: the *m. infraspinatus* acts as a lateral collateral support for the shoulder (along with the *m. subscapularis* on the medial scapula). The mechanical advantage would not have shifted greatly, if at all, given the close proximity to the joint centre (the gleno-humeral joint). The reorientation of the *m. infraspinatus* between the usual ungulate arrangement (i.e. contained within the infraspinous fossa) to the currently recognised tapir condition may have brought the line of action for the *m. infraspinatus* directly over the gleno-humeral joint, conferring optimal stability for the proximal forelimb joint. This could thus be beneficial for these relatively large, manoeuvrable, closed-habitat specialists, especially during rapid bursts of speed. Digitally modelling this arrangement in a virtual musculoskeletal setup would enable this hypothesis to be tested more rigorously. The 'invasion' of the supraspinous region of the scapula by the *m. infraspinatus*

seems to have occurred early on in *Tapirus* evolution, and evidently this shift in muscle origination site(s) was not deleterious to the functionality of the limb. As such, the arrangement of muscles and presence of the supraspinous ridge may represent evidence of a non-adaptive morphological change which did not improve nor impede fitness for early *Tapirus* members, and has persisted into the modern day.

## Conclusion

The anatomy of ungulates with non-veterinary associations has often been inferred from assumptions drawn from veterinary models, such as horses (*Equus*), bovids (*Bos*, *Capra*, *Ovis*) and suids (*Sus*). In this study I have demonstrated the importance for species-specific gross dissection for a fuller understanding of the locomotor musculoskeletal system of an enigmatic ungulate: the tapir. Moreover, this work highlights the potential for post-cranial osteological features of the forelimb of tapirids (namely the 'supraspinous ridge') to be used as discrete characters for phylogenetic reconstruction. Given the paucity of large-scale comparative anatomical studies on herbivorous mammals, particularly in their locomotor anatomy, this study represents a timely reminder for anatomists, veterinarians, and palaeontologists that using veterinary model organisms to infer form or function in non-model systems must be performed with care. In particular, greater efforts should be undertaken to broaden the pool of comparative subjects (i.e. taxa) which researchers and technicians can compare their own (often novel) materials with. This study on the scapula and shoulder musculature of tapirids has uncovered previously undescribed variation in the limb anatomy (both osteological and muscular), and the results could easily be used within a comparative framework to investigate locomotor histories of perissodactyls by enabling more accurate digital modelling. Additionally, the results offered here present lines of inquiry which until now represented "unknown unknowns"; these include, but are not limited to: the (geological) timing of muscle origin changes; the biomechanical function (or benefits) of the dual origin of the *m. infraspinatus* in *Tapirus*; and the more far-reaching question of functional inferences being made for extinct taxa that may be founded on erroneous information if based solely on the musculoskeletal system of veterinary model groups.

**Acknowledgements:** I would like to thank the following for their provision of specimens and workspace for this study: Sandra Nauwelaerts, Ellen Goosenaerts, Denise Vogel, Chris Van Ginneken (UAntwerpen); Chris Conroy (MVZ); Christiane Funk (ZMB); Eleanor Hoeger (AMNH); Pepijn Kamminga (RMNH); Josephine Lesur (MNHN); Luc Tyteca (MEO); Frank Zachos (NHMW); Richard Hulbert, Jeanette Pirlo, Rachel Narducci (FLMNH); Chris Widga, Steve Wallace (ETMNH); John Demboski, Andie Carrillo, Kristen MacKenzie, Garth Spellman (DMNS); Mason Kirkland (LSU); Liza Dadone and the staff of Cheyenne Mountain Zoo; Francis Vercammen and the staff of Antwerp Zoo (KMDA); Alex Larsson, Bim Boijsen, Linda Berggren and the staff of Kolmården Wildlife Park. I would also like to specifically thank Martha MacMillan, Eleesha Annear, and Brianna McHorse for their hands-on assistance during dissections, and both Peter Aerts and Federico Banfi for their assistance in translating foreign texts. Extended thanks to Christine Böhmer (Editor) and both Eloy Gálvez-López and Cyril Etienne (reviewers) for their constructive comments during review. This study was financially supported by doctoral (11Y7615N) and post-doctoral (12V8422N) fellowships from the FWO (Fonds Wetenschappelijk Onderzoek), an FWO Short-Stay Travel Grant (Denver, 2022; K207322N), and a Company of Biologists Travel Grant (Kolmården, 2023).

## References


Bai, B., Meng, J., Mao, F. Y., Zhang, Z. Q., & Wang, Y. Q. (2019). A new early Eocene deperetellid tapiroid illuminates the origin of Deperetellidae and the pattern of premolar molarization in Perissodactyla. *PLoS ONE*, *14*(11), 1–26. https://doi.org/10.1371/journal.pone.0225045

Bai, B., Wang, Y.-Q., Mao, F. Y., & Meng, J. (2017). New material of Eocene Helaletidae (Perissodactyla, Tapiroidea) from the Irdin Manha Formation of the Erlian Basin, Inner Mongolia, China and comments on related localities of the Huheboerhe Area. *American Museum Novitates*, *3878*, 1–44. https://doi.org/10.1206/3878.1

Bapst, D. W. (2012). paleotree: an R package for paleontological and phylogenetic analyses of evolution. *Methods in Ecology and Evolution*, *3*(5), 803–807. https://doi.org/10.1111/j.2041-210X.2012.00223.x

Berta, A., Sumich, J. L., Kovacs, K. M., Folkens, P. A., & Adam, P. J. (2015). Pinniped Evolution and Systematics. In A. Berta, J. L. Sumich, K. M. Kovacs, P. A. Folkens, & P. J. Adam (Eds.), *Marine Mammals: Evolutionary Biology* (3rd ed., pp. 35–61). Academic Press. https://doi.org/10.1016/b978-0-12-397002-2.00003-x

Berta, A., & Wyss, A. R. (1994). Pinniped phylogeny. *Proceedings of the San Diego Society of Natural History*, *29*, 33–56.

Böhmer, C., Theil, J.-C., Fabre, A.-C., & Herrel, A. (2020). Atlas of Terrestrial Mammal Limbs. In C. Böhmer, J.-C. Theil, A.-C. Fabre, & A. Herrel (Eds.), *Atlas of Terrestrial Mammal Limbs* (1st ed.). CRC Press. https://doi.org/10.1201/b22115

Bressou, C. (1961). La myologie du tapir (*Tapirus indicus* L.). *Mammalia*, *25*(3), 358–400. https://doi.org/10.1515/mamm.1961.25.3.358

Budras, K.-D., Sack, W. O., & Rock, S. (2012). Thoracic Limb. In K.-D. Budras, W. O. Sack, & S. Rock (Eds.), *Anatomy of the Horse* (Sixth, pp. 4–14). Schlutersche.

Campbell, B. (1936). The comparative myology of the forelimb of the hippopotamus, pig and tapir. *American Journal of Anatomy*, *59*(2), 201–247.

Constantinescu, G. M., Habel, R. E., Hillebrand, A., Sack, W. O., Schaller, O., Simoens, P., & de Vos, N. R. (2012). Osteologia. In G. M. Constantinescu & O. Schaller (Eds.), *Illustrated Veterinary Anatomical Nomenclature* (Third, pp. 10–62). Enke.

Cozzuol, M. A., Clozato, C. L., Holanda, E. C., Rodrigues, F. H. G., Nienow, S., de Thoisy, B., Redondo, R. A. F., & Santos, F. R. (2013). A new species of tapir from the Amazon. *Journal of Mammalogy*, *94*(6), 1331–1345. https://doi.org/10.1644/12-MAMM-A-169.1

Cuff, A. R., Sparkes, E. L., Randau, M., Pierce, S. E., Kitchener, A. C., Goswami, A., & Hutchinson, J. R. (2016). The scaling of postcranial muscles in cats (Felidae) I: forelimb, cervical, and thoracic muscles. *Journal of Anatomy*, *229*(1), 128–141. https://doi.org/10.1111/joa.12477

Deutsch, A. R., Dickinson, E., Leonard, K. C., Pastor, F., Muchlinski, M. N., & Hartstone-Rose, A. (2020). Scaling of Anatomically Derived Maximal Bite Force in Primates. *Anatomical Record*, *303*(7). https://doi.org/10.1002/ar.24284

Diedrich, C. G. (2012). Late Pleistocene *Crocuta crocuta spelaea* (Goldfuss 1823) populations from the Emscher River terrace open air hyena den near Bottrop and other sites in NW Germany: Their bone accumulations along rivers in lowland mammoth steppe environments and scavenging activities on woolly rhinoceros. *Quaternary International*, *276–277*. https://doi.org/10.1016/j.quaint.2011.07.046

Diniz, J. A. R. A., Falcão, B. M. R., Rocha, E. F., De Souza, J. G., Da Nobrega Carreiro, A., Medeiros, G. X., & De Menezes, D. J. A. (2018). Anatomical description of the forelimb muscles of the brown-throated sloth (*Bradypus variegatus*). *Acta Scientiae Veterinariae*, *46*(1). https://doi.org/10.22456/1679-9216.85986

English, A. W. M. (1976). Functional anatomy of the hands of fur seals and sea lions. *American Journal of Anatomy*, *147*(1), 1–17. https://doi.org/10.1002/aja.1001470102

English, A. W. M. (1977). Structural correlates of forelimb function in fur seals and sea lions. *Journal of Morphology*, *151*(3), 325–352. https://doi.org/10.1002/jmor.1051510303

Etienne, C., Houssaye, A., & Hutchinson, J. R. (2021). Limb myology and muscle architecture of the Indian rhinoceros *Rhinoceros unicornis* and the white rhinoceros *Ceratotherium simum* (Mammalia: Rhinocerotidae). *PeerJ*, *9*, e11314. https://doi.org/10.7717/peerj.11314

Fabre, A. C., Perry, J. M. G., Hartstone-Rose, A., Lowie, A., Boens, A., & Dumont, M. (2018). Do Muscles Constrain Skull Shape Evolution in Strepsirrhines? *Anatomical Record*, *301*(2), 291–310. https://doi.org/10.1002/ar.23712

Falconi-Briones, F. A., Naranjo, E. J., Reyna-Hurtado, R., Spínola, M., Enríquez-Rocha, P., & Medellín, R. A. (2022). Habitat use and activity patterns of ungulates in a tropical rainforest of southern México. *Therya*, *13*(2), 171–182. https://doi.org/10.12933/therya-22-1167

Flinn, E. B., Strickland, B. K., Demarais, S., & Christiansen, D. (2013). Age and gender affect epiphyseal closure in white-tailed deer. *Southeastern Naturalist*, *12*(2). https://doi.org/10.1656/058.012.0205

Franzen, J. L. (2010). Pseudo Horses and Relatives of Horses. In *The Rise of Horses: 55 Million Years of Evolution* (pp. 145–164). Johns Hopkins University Press.

Gardiner, J. D., Behnsen, J., & Brassey, C. A. (2018). Alpha shapes: Determining 3D shape complexity across morphologically diverse structures. *BMC Evolutionary Biology*, *18*(1), 184 (2018). https://doi.org/10.1186/s12862-018-1305-z

Grandi, F., Del Valle, H., Cáceres, I., Rodríguez-Salgado, P., Oms, O., Fernández-Jalvo, Y., García, F., Campeny, G., & Gómez de Soler, B. (2023). Exceptional preservation of large fossil vertebrates in a volcanic setting (Camp dels Ninots, Spain). *Historical Biology*, *35*(7), 1234–1249. https://doi.org/10.1080/08912963.2022.2085570

Graziotti, G. H., Chamizo, V. E., Ríos, C., Acevedo, L. M., Rodríguez-Menéndez, J. M., Victorica, C., & Rivero, J. L. L. (2012). Adaptive functional specialisation of architectural design and fibre type characteristics in agonist shoulder flexor muscles of the llama, *Lama glama*. *Journal of Anatomy*, *221*(2), 151–163. https://doi.org/10.1111/j.1469-7580.2012.01520.x

Großmann, M., Sánchez-Villagra, M. R., & Maier, W. (2002). On the development of the shoulder girdle in Crocidura russula (Soricidae) and other placental mammals: Evolutionary and functional aspects. *Journal of Anatomy*, *201*(5). https://doi.org/10.1046/j.0021-8782.2002.00105.x

Groves, C., & Grubb, P. (2011). Tapiridae. In C. Groves & P. Grubb (Eds.), *Ungulate taxonomy* (1st ed., Issue 09, pp. 18–20). Johns Hopkins University Press. https://doi.org/10.5860/choice.49-5062

Handa, N., Izuho, M., Takahashi, K., Iizuka, F., Tsogtbaatar, B., Gunchinsuren, B., Odosuren, D., & Ishitseren, L. (2022). The woolly rhinoceros (*Coelodonta antiquitatis*) from Ondorkhaan, eastern Mongolia. *Boreas*, *51*(3), 584–605. https://doi.org/10.1111/bor.12582

Hartstone-Rose, A., Dickinson, E., Deutsch, A. R., Worden, N., & Hirschkorn, G. A. (2022). Masticatory muscle architectural correlates of dietary diversity in Canidae, Ursidae, and across the order Carnivora. *Anatomical Record*, *305*(2), 477–497. https://doi.org/10.1002/ar.24748

Hartstone-Rose, A., Perry, J. M. G., & Morrow, C. J. (2012). Bite Force Estimation and the Fiber Architecture of Felid Masticatory Muscles. *Anatomical Record*, *295*(8), 1336–1351. https://doi.org/10.1002/ar.22518

Holanda, E. C., Ferigolo, J., & Ribeiro, A. M. (2011). New Tapirus species (Mammalia: Perissodactyla: Tapiridae) from the upper Pleistocene of Amazonia, Brazil. *Journal of Mammalogy*, *92*(1), 111–120. https://doi.org/10.1644/10-MAMM-A-144.1

Holanda, E. C., & Ferrero, B. S. (2013). Reappraisal of the genus *Tapirus* (Perissodactyla, Tapiridae): systematics and phylogenetic affinities of the South American tapirs. *Journal of Mammalian Evolution*, *20*(1), 33–44. https://doi.org/10.1007/s10914-012-9196-z

Holanda, E. C., Ribeiro, A. M., & Ferigolo, J. (2012). New material of *Tapirus* (Perissodactyla: Tapiridae) from the Pleistocene of southern Brazil. *Revista Mexicana de Ciencias Geologicas*, *29*(2), 308–318.

Hulbert, R. C. (2005). Late Miocene *Tapirus* (Mammalia, Perissodactyla) from Florida, with description of a new species, *Tapirus webbi*. *Bulletin of the Florida Museum of Natural History*, *45*(4), 465–494.

Hulbert, R. C. (2010). A new early Pleistocene tapir (Mammalia: Perissodactyla) from Florida, with a review of Blancan tapirs from the state. *Bulletin of the Florida Museum of Natural History*, *49*(3), 67–126.

Kavanagh, K. D., Bailey, C. S., & Sears, K. E. (2020). Evidence of five digits in embryonic horses and developmental stabilization of tetrapod digit number. *Proceedings of the Royal Society B: Biological Sciences*, *287*(1920), 20192756. https://doi.org/10.1098/rspb.2019.2756

King, J. E. (1983). *Seals of the World* (2nd ed.). British Museum of Natural History.

Law, C. J., Blackwell, E. A., Curtis, A. A., Dickinson, E., Hartstone-Rose, A., & Santana, S. E. (2022). Decoupled evolution of the cranium and mandible in carnivoran mammals. *Evolution*, *76*(12), 2959–2974. https://doi.org/10.1111/evo.14578

Liebich, H.-G., & König, H. E. (2020). Veterinary Anatomy of Domestic Animals. In Hans-Georg Liebich & Horst Erich König (Eds.), *Veterinary Anatomy of Domestic Animals* (7th ed.). Elsevier. https://doi.org/10.1055/b-007-167437

Liebich, H.-G., Konig, H. E., & Maierl, J. (2007). Forelimb or thoracic limb (membra thoracica). In H. E. Konig & H.-G. Liebich (Eds.), *Veterinary Anatomy of Domestic Animals: Textbook and Colour Atlas* (Third, pp. 145–214). Schlutersche.

MacLaren, J. A., Hulbert, R. C., Wallace, S. C., & Nauwelaerts, S. (2018). A morphometric analysis of the forelimb in the genus *Tapirus* (Perissodactyla: Tapiridae) reveals influences of habitat, phylogeny and size through time and across geographical space. *Zoological Journal of the Linnean Society*, *184*(2), 499–515.

MacLaren, J. A., & McHorse, B. K. (2020). Comparative forelimb myology and muscular architecture of a juvenile Malayan tapir (*Tapirus indicus*). *Journal of Anatomy*, *236*(1), 85–97. https://doi.org/10.1111/joa.13087

MacLaren, J. A., & Nauwelaerts, S. (2016). A three-dimensional morphometric analysis of upper forelimb morphology in the enigmatic tapir (Perissodactyla: *Tapirus*) hints at subtle variations in locomotor ecology. *Journal of Morphology*, *277*(11), 1469–1485.

MacLaren, J. A., & Nauwelaerts, S. (2020). Modern Tapirs as Morphofunctional Analogues for Locomotion in Endemic Eocene European Perissodactyls. *Journal of Mammalian Evolution*, *27*(2), 245–263. https://doi.org/10.1007/s10914-019-09460-1

Marchi, D., Leischner, C. L., Pastor, F., & Hartstone-Rose, A. (2018). Leg Muscle Architecture in Primates and Its Correlation with Locomotion Patterns. *Anatomical Record*, *301*(3), 515–527. https://doi.org/10.1002/ar.23745

Martini, P., Schmid, P., & Costeur, L. (2018). Comparative morphometry of Bactrian Camel and Dromedary. *Journal of Mammalian Evolution*, *25*(2), 407–425. https://doi.org/10.1007/S10914-017-9386-9

Maynard Smith, J., & Savage, R. J. G. (1956). Some locomotory adaptations in mammals. *Journal of the Linnean Society of London, Zoology*, *42*(288), 603–622. https://doi.org/10.1111/j.1096-3642.1956.tb02220.x

Murie, J. (1872). On the Malayan tapir, *Rhinochoerus sumatranus* (Gray). *Journal of Anatomy and Physiology*, *6*, 131–169.

Nyakatura, J. A., & Fischer, M. S. (2011). Functional morphology of the muscular sling at the pectoral girdle in tree sloths: Convergent morphological solutions to new functional demands? *Journal of Anatomy*, *219*(3), 360–374. https://doi.org/10.1111/j.1469-7580.2011.01394.x

Nyakatura, J. A., Melo, K., Horvat, T., Karakasiliotis, K., Allen, V. R., Andikfar, A., Andrada, E., Arnold, P., Lauströer, J., Hutchinson, J. R., Fischer, M. S., & Ijspeert, A. J. (2019). Reverse-engineering the locomotion of a stem amniote. *Nature*, *565*(7739), 351–355. https://doi.org/10.1038/s41586-018-0851-2

Olsen, S. J. (1960). Age and faunal relationship of *Tapiravus* remains from Florida. *Journal of Paleontology*, *34*(1), 164–167. https://www.jstor.org/stable/1300997

Olson, R. A., Glenn, Z. D., Cliffe, R. N., & Butcher, M. T. (2018). Architectural properties of sloth forelimb muscles (Pilosa: Bradypodidae). *Journal of Mammalian Evolution*, *25*(4), 573–588. https://doi.org/10.1007/s10914-017-9411-z

Onwuama, K. T., Salami, S. O., Kigir, E. S., & Jaji, A. Z. (2021). Gross Anatomical Studies on the Hind Limb of the West African Giraffe (*Giraffa camelopardalis peralta*). *Veterinary Medicine International*, *2021*, 8818525. https://doi.org/10.1155/2021/8818525

Padilla, M., Dowler, R. C., & Downer, C. C. (2010). *Tapirus pinchaque* (Perissodactyla: Tapiridae). *Mammalian Species*, *42*(1), 166–182.

Pampush, J. D., Winchester, J. M., Morse, P. E., Vining, A. Q., Boyer, D. M., & Kay, R. F. (2016). Introducing molaR: a New R Package for Quantitative Topographic Analysis of Teeth (and Other Topographic Surfaces). *Journal of Mammalian Evolution*, *23*(4), 397–412. https://doi.org/10.1007/s10914-016-9326-0

Pereira, S. G., Santos, A. L. Q., Borges, D. C. S., de Souza, R. R., & Quaioz, P. R. (2015). Anatomia óssea e muscular do cíngulo escapular e braço de *Tapirus terrestris* (Perissodactyla: Tapiridae). *Ciencia Animal Brasileira*, *16*(2), 268–278. https://doi.org/10.1590/1089-6891v16i228130

Pereira, S. G., Santos, A. L. Q., Borges, D. C. S., Ribeiro, P. R. Q., & Rodrigues de Souza, R. (2017). Bone and muscular anatomy of the forearm and hand in *Tapirus terrestris* (Perissodactyla, Tapiridae). *Biotemas*, *30*(2), 35–41.

Qiu, Z., Yan, D., & Sun, B. (1991). A new genus of Tapiridae from Shanwang, Shandong. *Vertebrata Palasiatica*, *29*(2), 119–135.

R Core Team. (2020). *R: a language and environment for statistical computing*. R Foundation for Statistical Computing.

RC Epic Games Slovakia. (2023). *Reality Capture* (1.2.1.116300). Epic Games Slovakia.

Regnault, S., & Pierce, S. E. (2018). Pectoral girdle and forelimb musculoskeletal function in the echidna (*Tachyglossus aculeatus*): insights into mammalian locomotor evolution. *Royal Society Open Science*, *5*(11), 181400. https://doi.org/10.1098/rsos.181400

Revell, L. J. (2012). phytools: an R package for phylogenetic comparative biology (and other things). *Methods in Ecology and Evolution*, *3*(2), 217–223. https://doi.org/10.1111/j.2041-210X.2011.00169.x

Rogers, C. W., Gee, E. K., & Dittmer, K. E. (2021). Growth and bone development in the horse: When is a horse skeletally mature? In *Animals* (Vol. 11, Issue 12). https://doi.org/10.3390/ani11123402

RStudio Team. (2020). *RStudio: Integrated Development for R*. RStudio, PBC.

Smith, H. F., Adrian, B., Koshy, R., Alwiel, R., & Grossman, A. (2020). Adaptations to cursoriality and digit reduction in the forelimb of the African wild dog (*Lycaon pictus*). *PeerJ*, *8*, e9866. https://doi.org/10.7717/peerj.9866

Spradley, J. P., Pampush, J. D., Morse, P. E., & Kay, R. F. (2017). Smooth operator: The effects of different 3D mesh retriangulation protocols on the computation of Dirichlet normal energy. *American Journal of Physical Anthropology*, *163*(1), 94–109. https://doi.org/10.1002/ajpa.23188

Toledo, N., Bargo, M. S., & Vizcaíno, S. F. (2013). Muscular reconstruction and functional morphology of the forelimb of Early Miocene sloths (Xenarthra, Folivora) of Patagonia. *The Anatomical Record*, *296*(2), 305–325. https://doi.org/10.1002/ar.22627

Tong, H. W., & Wang, X. M. (2014). Juvenile skulls and other postcranial bones of *Coelodonta nihowanensis* from Shanshenmiaozui, Nihewan Basin, China. *Journal of Vertebrate Paleontology*, *34*(3), 710–724. https://doi.org/10.1080/02724634.2013.814661

Van Der Made, J., & Stefanovic, I. (2006). A small tapir from the Turolian of Kreka (Bosnia) and a discussion on the biogeography and stratigraphy of the Neogene tapirs. *Neues Jahrbuch Fur Geologie Und Palaontologie - Abhandlungen*, *240*(2), 207–240. https://doi.org/10.1127/njgpa/240/2006/207

Van Houtven, K., & MacLaren, J. A. (2019). Shoulder-blade Runners: Utility of the Scapula Fossa Ratio to Investigate Locomotor Evolution in Equids (Mammalia: Perissodactyla). *Journal of Morphology*, *280*(S1), S232.

Vélez-García, J. F., Ramírez-Arias, J. C., & Duque-Parra, J. E. (2018). Gross anatomy of the intrinsic muscles of the scapular and humeral joint regions in crab-eating fox (*Cerdocyon thous*, Linnaeus 1776). *Acta Scientiarum - Biological Sciences*, *40*(1), 1–7. https://doi.org/10.4025/actascibiolsci.v40i1.37861

Waldman, E., Gonzalez, Y., Flynn, J. J., & Tseng, Z. J. (2023). Dental topographic proxies for ecological characteristics in carnivoran mammals. *Journal of Anatomy*, *242*(4), 627–641. https://doi.org/10.1111/joa.13806

Wareing, K., Tickle, P. G., Stokkan, K. A., Codd, J. R., & Sellers, W. I. (2011). The musculoskeletal anatomy of the reindeer (*Rangifer tarandus*): fore- and hindlimb. *Polar Biology*, *34*(10), 1571–1578. https://doi.org/10.1007/s00300-011-1017-y

Witmer, L. M. (1995). The Extant Phylogenetic Bracket and the importance of reconstructing soft tissues in fossils. In J. J. Thomason (Ed.), *Functional Morphology in Vertebrate Paleontology* (pp. 19–33). Cambridge University Press.

Wood, A. R., Bebej, R. M., Manz, C. L., Begun, D. L., & Gingerich, P. D. (2011). Postcranial functional morphology of *Hyracotherium* (Equidae, Perissodactyla) and locomotion in the earliest horses. *Journal of Mammalian Evolution*, *18*(1), 1–32. https://doi.org/10.1007/s10914-010-9145-7

## Figure Legends

**Figure 1**. Lateral shoulder musculature from dissection of (a) *Tapirus indicus* (Qadira, KMDA), (b) *T. terrestris* (Thorbjorn, Kolmården), and (c) *T. pinchaque* (Carlotta, DMNS). Photographs (top) presented alongside diagrams illustrating locations of specific muscles at three stages of muscle removal. From the left: lateral muscles intact, *m. deltoideus* removed in two cases; *m. supraspinatus* removed; *m. infraspinatus* reflected revealing scapular spine.

**Figure 2.** Diagram illustrating the methodology used for quantifying two-dimensional scapular fossa ratio (2D-SFR). (a) Rendered 3D model of scapula (*Tapirus indicus* NHMW 1938) with cut-away to reveal cross-section, taken just prior to *tuber spinae scapulae*. (b) Measurements recorded for *m. supraspinatus* (light blue) and *m. infraspinatus* (purple) attachment regions in cross-section (dotted lines), with 2D-SFR equation adapted from MacLaren and Nauwelaerts (2016). (c) Exemplar cross-sections through scapulae of specimens from three extant species: *T. indicus* (NHMW 1938), *T. terrestris* (MEO 2204b) and *T. pinchaque* (MEO 2203a). Arrows denote the bony ridge delineating the epimysial border between *m. supraspinatus* and *m. infraspinatus* muscles.

**Figure 3.** Comparison of full scapulae from (A) *Tapirus indicus*, (B) *T. terrestris*, and (C) *T. pinchaque*, including silhouettes of pre-tuber cross-sections, and with approximate areas of muscle origin highlighted. (D) A composite phylogeny tracing the expression of the supraspinous ridge on the tapiromorph scapula through evolutionary time. Symbols and abbreviations: † = extinct species; Pal. = Palaeocene; Plio. = Pliocene; Plei. = Pleistocene.

**Figure 4.** Graphical results comparing 2D-CS (cross-sectional) scapular fossa ratios for seven *Tapirus* species. (a) Biplot comparing lengths of m. infraspinatus and m. supraspinatus origination sites from pre-tuber cross-sections (see Figure 2). (b) Boxplot comparing ranges and medians (black line) of 2D scapular fossa ratios. Box limits denote 95% confidence interval. *Tapirus indicus* exhibited the only significant difference in mean SFR

values ($p < 0.01$, derived from ANOVA and Tukey HSD post-hoc) compared to all other taxa in the study which were represented by more than a single complete scapula, here denoted with ***.

**Figure 5**. Lateral scapula surface topography comparisons across tapiromorph species. Images of scans (a-i+l; top) and Dirchelet's Normal Energy maps (a-i & l; bottom) for 3D scanned tapiromorph scapulae enable presence or absence of supraspinous ridge to be defined. Ridge is present on scapular spine in (a), present on the supraspinous fossa in (b-i), and is not visible in (j-l). Arrows provided to guide reader to the location of the supraspinous ridge on images of scans. Digital lighting was modified between scans to provide the best view of ridge. Angled light images captured in MeshLab using the 'lattice' shader from the Render menu with RGB colouration (255-255-225). DNE topographical complexity colours indicate elevated surfaces (red), depressed surfaces (blue) and neutral surfaces (yellows and greens). All right scapulae images were mirrored to face left for ease of comparison. Symbols and abbreviations: † = extinct species. Specimens: (a) NHMW 1938, (b) RMNH 43495, (c) MEO 2204b, (d) MEO 2203a, (e) ETMNH 8187, (f) UF 32084, (g) UF 206876, (h) UF 67539, (i) UF 14064, (j) LSU V-2455, (k) HLMD-Me 16000, (l) DMNS 15399. Institutional abbreviations are provided in the Supplementary Information 6.

**Figure 6.** Comparison of lateral scapula surfaces for a range of ungulate mammals (plus one carnivoran), demonstrating absence of 'supraspinous ridge' morphology in all groups except tapirids. (a) *Tapirus indicus* (NHMW 1938; top) and *T. terrestris* (RMNH 12913); (b) *Dicerorhinus sumatrensis* (MNHN ZM AC 1887-432; left) and *Ceratotherium simum* (MEO 2208c; right); (c) *Sifrhippus grangeri* (UM 115547 left), *Archaeohippus blackbergi* (UF 161188; centre); *Equus kiang* (NHMW 7222; right); (d) *Propalaeotherium hassiacum* (GMH-XIV-4545; left) and *Palaeotherium medium* (NHMUK PV OR 25336); (e) *Dicotyles tajacu* (MEO uncatalogued) (f) *Potamochoerus porcus* (IRSNB 12111); (g) *Eumetopias jubatus* (UWBM 39483). Left scapulae used for comparison where possible; image mirrored for right scapulae for ease of comparison.

758 **Figure 7**. Boxplot of scapula fossa ratio results from taxa in MacLaren and Nauwelaerts (2016; Figure 3),
759 adjusted after the findings of the present study. Solid black line denotes median, with black circles denoting
760 outliers.

761 **Tables**

762 **Table 1.** List of cadaveric specimens inspected as part of this study. Specimens considered skeletally mature
763 at two years.

| Specimen Name | Sex | Genus | Species | Age | Location |
|---|---|---|---|---|---|
| Kamal | M | *Tapirus* | *indicus* | 6 years | Antwerp Zoo (KMDA), Belgium |
| Qadira | F | *Tapirus* | *indicus* | 5 months | Antwerp Zoo (KMDA), Belgium |
| Torbjörn | M | *Tapirus* | *terrestris* | 3 years | Kolmården Zoo, Sweden |
| Carlotta | F | *Tapirus* | *pinchaque* | 28 years | Cheyenne Mountain Zoo, CO, USA |
| Cofan | M | *Tapirus* | *pinchaque* | 18 years | Cheyenne Mountain Zoo, CO, USA |

764

765

766 **Table 2.** Results of Welch's one-way analysis of variance (ANOVA) and pairwise post-hoc t-tests for
767 significant differences (p-values corrected using Holm-Bonferroni) in two-dimensional cross-sectional scapula
768 fossa ratios of *Tapirus* species. Degrees of freedom (df) listed alongside F-statistic (F) and overall significance
769 of the model (p-value; alpha = 0.05).

| **One-way analysis of means (not assuming equal variance)** | | | | |
|---|---|---|---|---|
| **Welch's F** | **Numerator df** | | **Denominator df** | **p-value** |
| 15.316 | 4.000 | | 5.256 | 0.004 |
| **Pairwise comparisons using t-tests (p-values corrected using Holm-Bonferroni)** | | | | |
| **Species** | ***Tapirus indicus*** | ***Tapirus bairdii*** | ***Tapirus pinchaque*** | ***Tapirus terrestris*** |
| *Tapirus indicus* | - | | | |
| *Tapirus bairdii* | 0.001 | - | | |
| *Tapirus pinchaque* | 0.001 | 0.719 | - | |
| *Tapirus terrestris* | <0.001 | 0.018 | 0.054 | - |
| *Tapirus polkensis* | <0.001 | 0.007 | 0.016 | 0.196 |

770

771

772 **Figures**

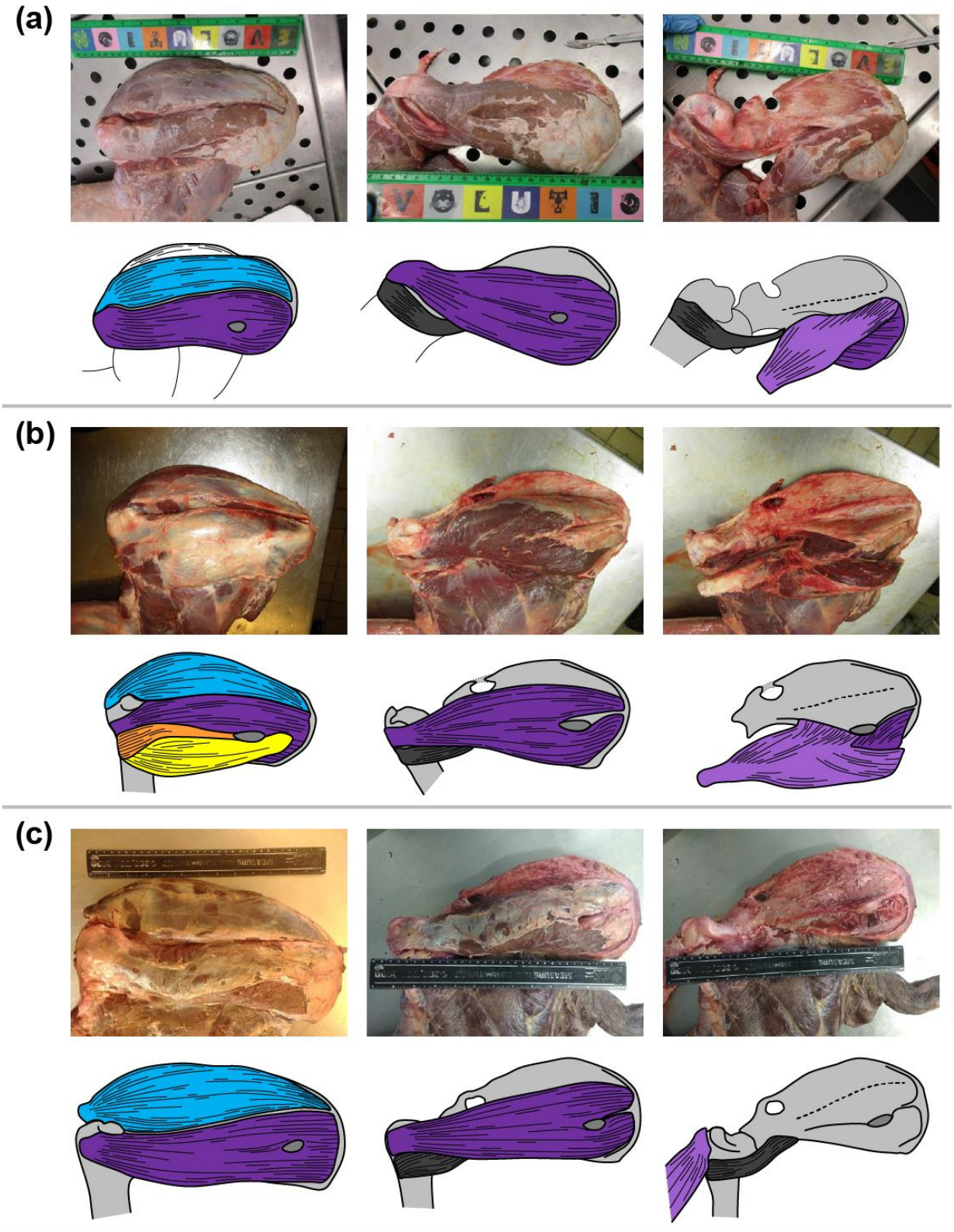


773

(a)

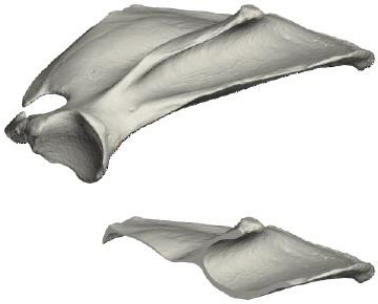

(b)

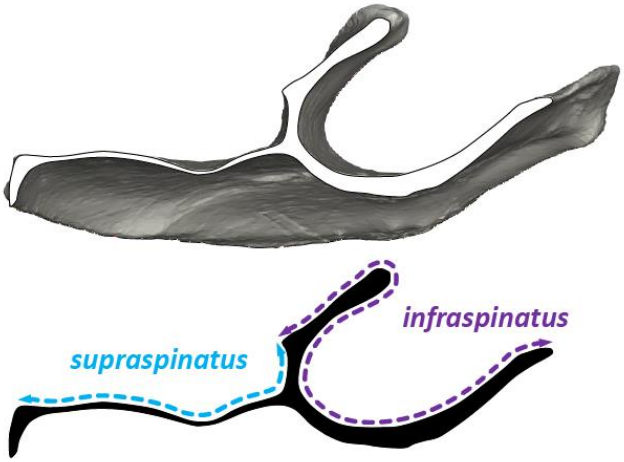


$$\text{2D Scapular Fossa Ratio} = \frac{Length_{supraspinatus}}{Length_{supraspinatus} + Length_{infraspinatus}}$$

(c)

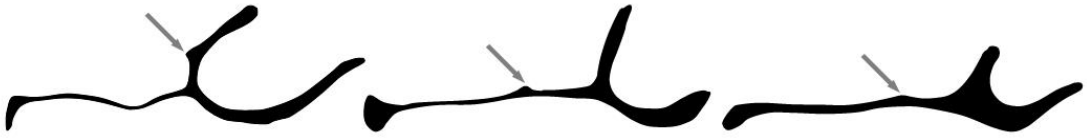

*Tapirus indicus* *Tapirus terrestris* *Tapirus pinchaque*

774

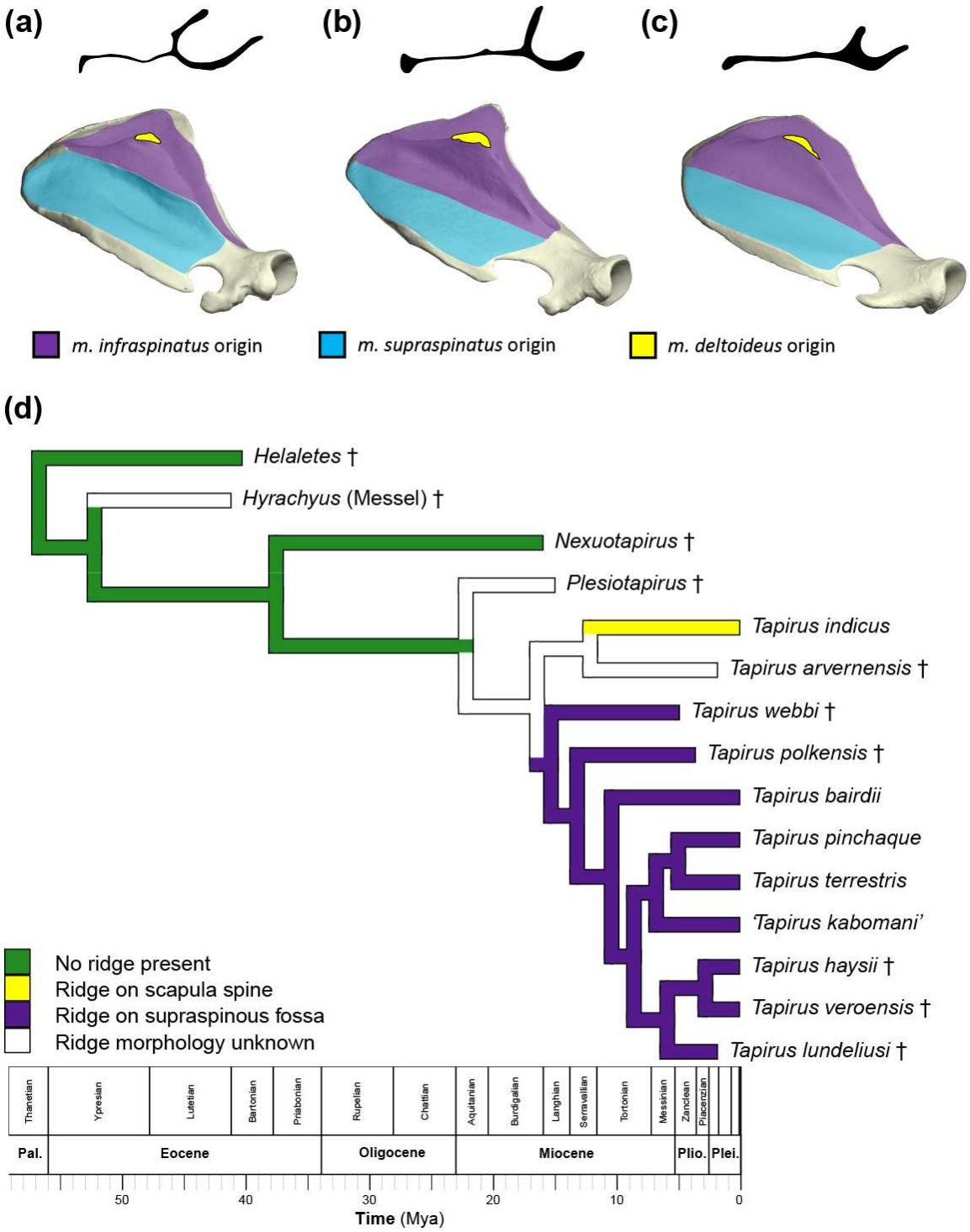
(a)
(b)
(c)
m. infraspinatus origin
m. supraspinatus origin
m. deltoideus origin
(d)
Helaletes †
Hyrachyus (Messel) †
Nexuotapirus †
Plesiotapirus †
Tapirus indicus
Tapirus arvernensis †
Tapirus webbi †
Tapirus polkensis †
Tapirus bairdii
Tapirus pinchaque
Tapirus terrestris
'Tapirus kabomani'
Tapirus haysii †
Tapirus veroensis †
Tapirus lundeliusi †
No ridge present
Ridge on scapula spine
Ridge on supraspinous fossa
Ridge morphology unknown
Thanetian
Ypresian
Lutetian
Bartonian
Priabonian
Rupelian
Chattian
Aquitanian
Burdigalian
Langhian
Serravallian
Tortonian
Messinian
Zanclean
Piacenzian
Pal.
Eocene
Oligocene
Miocene
Plio.
Plei.
50
40
30
20
10
0
Time (Mya)

775

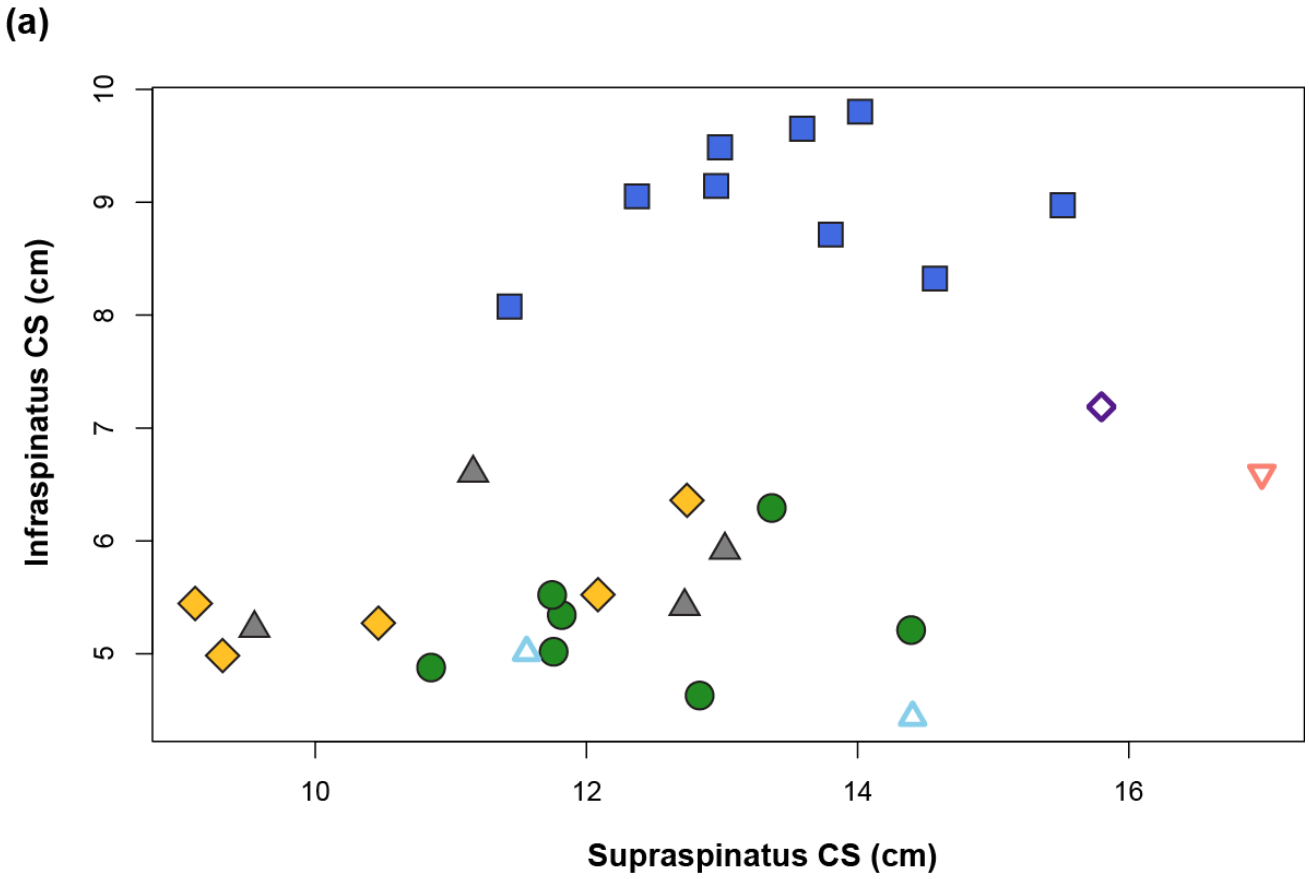
(a)
Infraspinatus CS (cm)
5
6
7
8
9
10
10
12
14
16
Supraspinatus CS (cm)

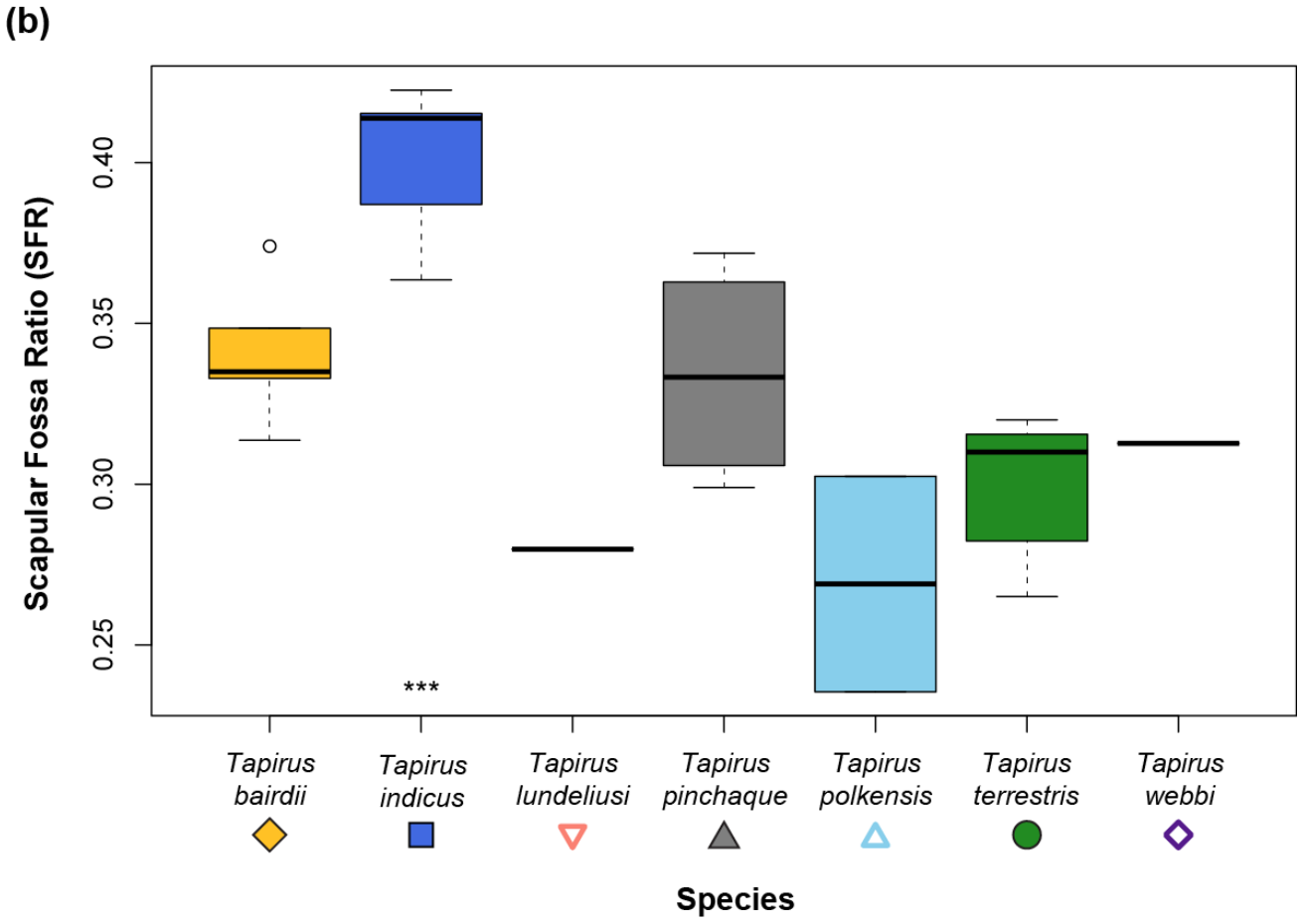
(b)
Scapular Fossa Ratio (SFR)
0.25
0.30
0.35
0.40
***
Tapirus bairdii
Tapirus indicus
Tapirus lundeliusi
Tapirus pinchaque
Tapirus polkensis
Tapirus terrestris
Tapirus webbi
Species

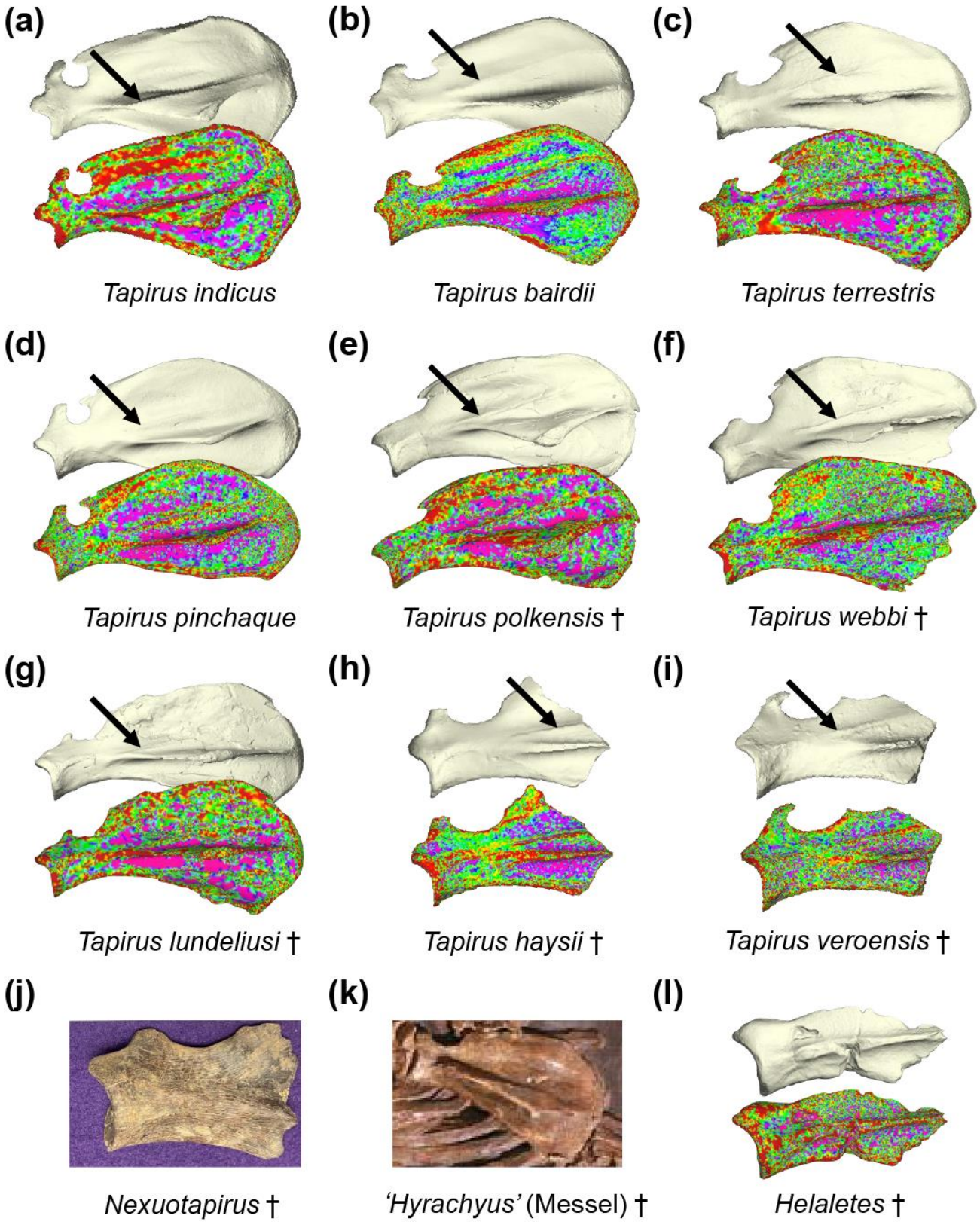
(a)
Tapirus indicus
(b)
Tapirus bairdii
(c)
Tapirus terrestris
(d)
Tapirus pinchaque
(e)
Tapirus polkensis †
(f)
Tapirus webbi †
(g)
Tapirus lundeliusi †
(h)
Tapirus haysii †
(i)
Tapirus veroensis †
(j)
Nexuotapirus †
(k)
'Hyrachyus' (Messel) †
(l)
Helaletes †

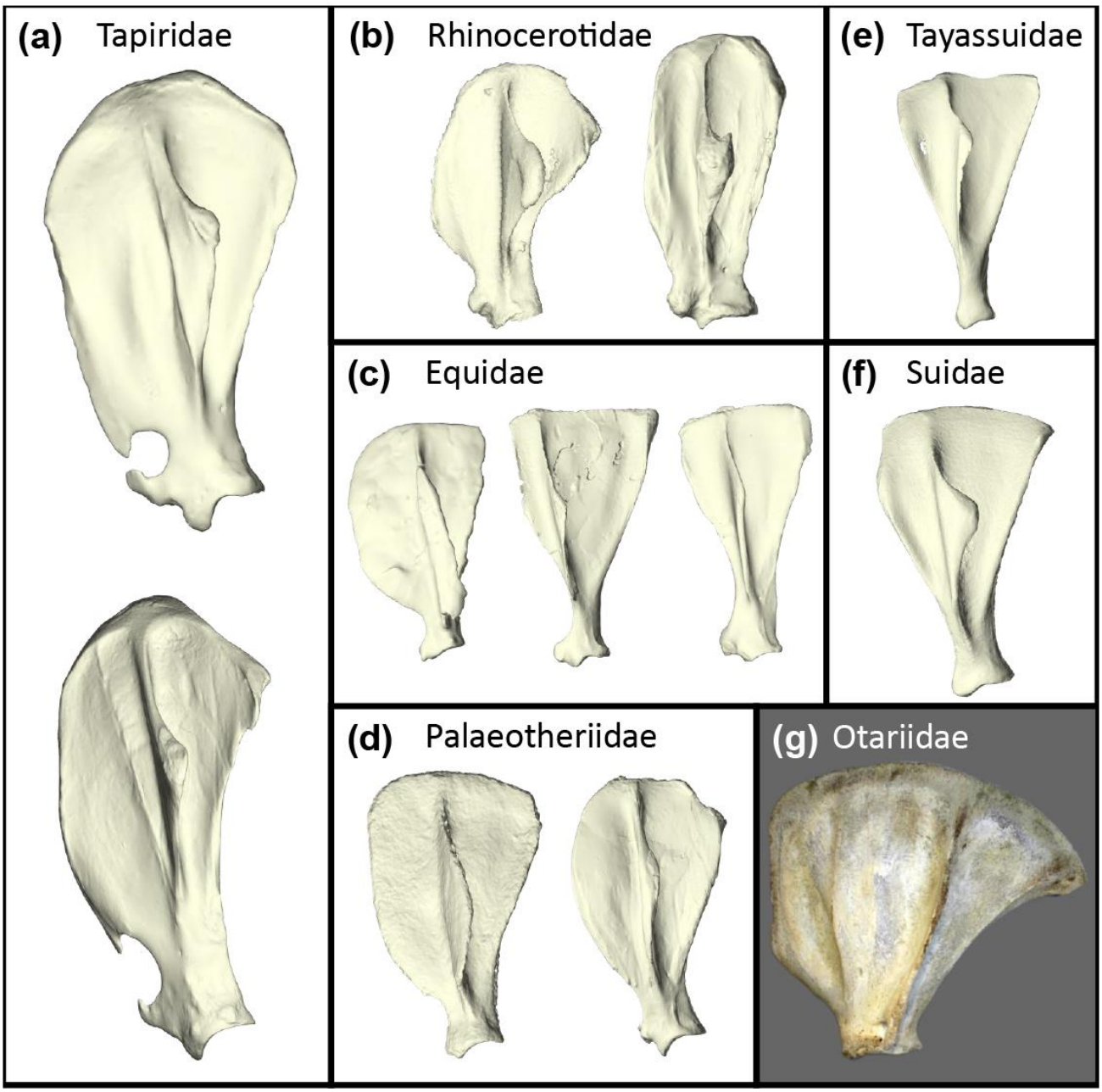
(a) Tapiridae
(b) Rhinocerotidae
(e) Tayassuidae
(c) Equidae
(f) Suidae
(d) Palaeotheriidae
(g) Otariidae

778

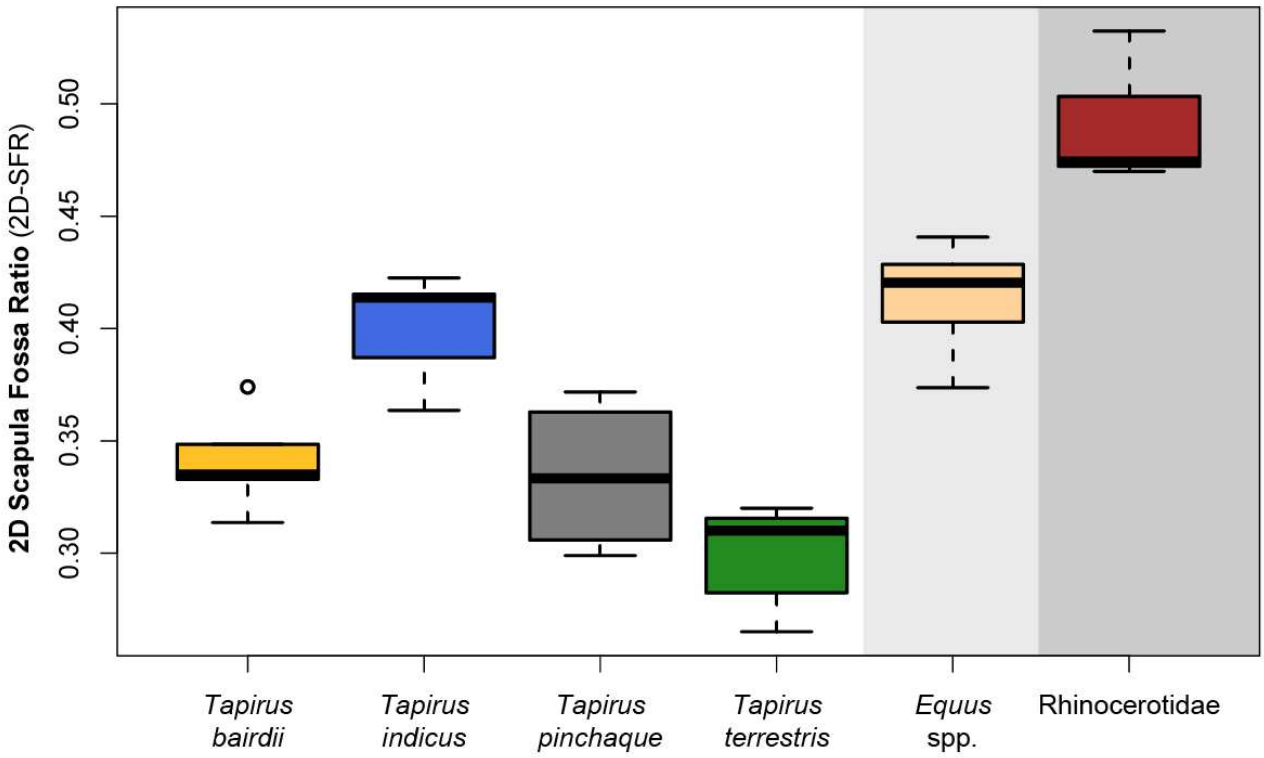
2D Scapula Fossa Ratio (2D-SFR)
0.30
0.35
0.40
0.45
0.50
Tapirus bairdii
Tapirus indicus
Tapirus pinchaque
Tapirus terrestris
Equus spp.
Rhinocerotidae

779